Dynamics of nanoscale polar regions and critical behavior of the uniaxial relaxor $Sr_{0.61}Ba_{0.39}Nb_2O_6:Co$

J. Banys,[1] J. Macutkevic,[1] R. Grigalaitis,[1] and W. Kleemann[2,*]
[1]*Faculty of Physics, Vilnius University, Sauletekio 9, 10222 Vilnius, Lithuania*
[2]*Angewandte Physik, Universität Duisburg-Essen, D-47048 Duisburg, Germany*
(Received 23 January 2005; published 12 July 2005)

The complex dielectric susceptibility of $Sr_{0.61}Ba_{0.39}Nb_2O_6:Co$ has been measured at frequencies $10^1 \leqslant f \leqslant 10^9$ Hz and temperatures $300 \leqslant T \leqslant 400$ K before and after poling. The high-frequency relaxation peak observed above the ferroelectric phase transition temperature, $T_c \approx 348$ K, is analyzed in terms of distribution functions of the relaxation time, $g(\tau)$, using Tikhonov regularization. It reveals the criticality of the largest relaxation time in agreement with activated dynamic scaling of the three-dimensional random-field Ising model. Differences of zero-field- and field-cooled $g(\tau)$ are discussed.

DOI: 10.1103/PhysRevB.72.024106 PACS number(s): 77.22.Ch, 64.70.Pf, 77.80.−e, 77.84.Dy

I. INTRODUCTION

Solving the relaxor enigma is still one of the most challenging problems in the physics of ferroelectrics. Ever since the discovery of the archetypical relaxor material $PbMg_{1/3}Nb_{2/3}O_3$ (PMN),[1] the origin of its key features—(i) huge frequency dispersion of the dielectric susceptibility in the Curie range above the transition temperature T_c, (ii) nonergodic behavior at low temperatures $T < T_c$, and (iii) virtually no symmetry breaking after zero-field cooling (ZFC) to below T_c—has been discussed controversially. Very probably and in accordance with long-standing propositions of Cross and co-workers[2,3] the appearance of fluctuating polar precursor clusters (*polar nanoregions*) at temperatures $T > T_c$ has to be considered as the primary signature of relaxor behavior.[4] Indeed, it appears plausible that polar nanoregions with a wide size distribution are at the heart of the observed giant polydispersivity,[5] which is observed in quite different systems like disordered solid solutions like PMN (Ref. 1) or PLZT (Ref. 2), or doped quantum paraelectrics like $SrTiO_3:Bi$ (Ref. 6).

Hence, finding out the microscopic origin of the polar precursor clusters is the key to understanding relaxor properties. Very probably, different mechanisms with different degrees of complexity have to be envisaged. They may range from purely statistical aggregation of polar centers in the sense of percolation theory [probably realized in the case of doped quantum paraelectrics like $SrTiO_3:Ca$ (Refs. 7 and 8)] to the appearance of weak ("exponentially rare") singularities within a dilution-induced Griffiths phase[9] (possibly realized in the case of solid solutions like PLZT, which reveal anomalies of the refractive index below the phase transition temperature T_c of the parent PZT phase irrespective of the amount of La doping.[10]). Apart from such very special mechanisms, however, the random-field (RF) mechanism[11] is supposed to be a widely applicable concept. Since spatial fluctuations of the RF's give rise to correlations between the fluctuating dipole moments, the formation of precursor clusters of mesoscopic size is expected in systems with charge disorder.[12–14]

Starting from the existence of polar nanoregions and assuming random interactions between them, a spherical random-bond random-field (SRBRF) theory[15] has successfully been introduced to describe the phase transition into a disordered low-T cluster glass phase. By assuming fully frustrated *superspin* interactions and dominance of these random bonds (RB's) over the RF's, it models the glassy freezing of mesoscopic nanoregions in cubic relaxors like PMN (Ref. 15) and PLZT (Ref. 16). Indeed, quite weak RF's are generally expected to act on the polar clusters, since only the fluctuations of the microscopic RF's are effective on a nanoscale. While cubic relaxors with nearly continuous order parameter have no chance to experience ferroelectric long-range order,[11] this must not be the case for random-field systems with a discrete order parameter. This is the reason why the well-known family of uniaxial relaxor crystals related to strontium-barium niobate, $Sr_xBa_{1-x}Nb_2O_6$ (SBN),[17] is considered as a prototypical three-dimensional (3D) random-field Ising-model (RFIM) system since recently.[18]

In contrast to the cubic perovskite family related to PMN,[1] the polarization of the SBN family is a single-component vector directed along the tetragonal c direction, which drives the point group from $4/mmm$ to $4mm$ at the phase transition into the low-T polar phase. Only at low temperatures is a slight tilt of the polarization out of the [001] direction observed, giving rise to a monoclinic structure (monoclinic point group m) below $T_0 \approx 70$ K.[19] At $T > T_0$, however, SBN is tetragonal on the average and thus belongs to an Ising model universality class rather than to a Heisenberg one as suggested for the PMN family.[12] Assuming the presence of quenched RF's, theory in this case predicts the existence of a phase transition into long-range order (LRO) within the RFIM universality class[11] preceded by a giant critical slowing-down above T_c. Hence, when approaching the ferroelectric state, the polar nanoregions, which are correlated by RF's in the paraelectric phase, should exhibit activated dynamics.[20]

Below T_c the polar nanoregions are expected to transform into polar LRO, provided that cooling is performed at a sufficiently low rate.[12] Recent studies of SBN and SBN:Ce have, indeed, evidenced that (i) the dielectric susceptibility probes clusters above and domains below T_c, respectively,[21] while (ii) the linear birefringence is a measure of polar pre-

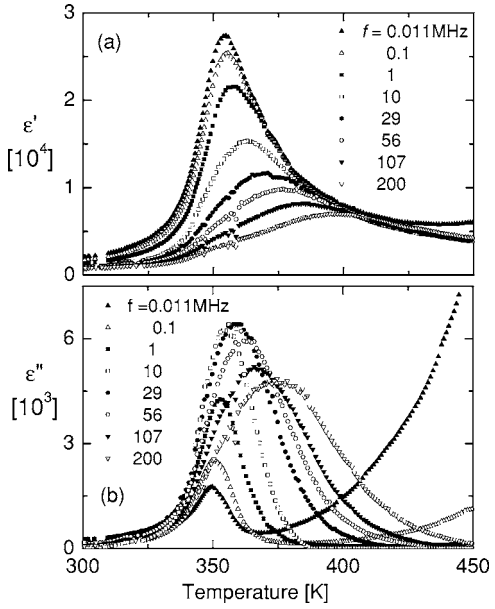

FIG. 1. Temperature dependence of the real (a) and imaginary parts (b) of the dielectric permittivity of unpoled SBN:Co at different frequencies.

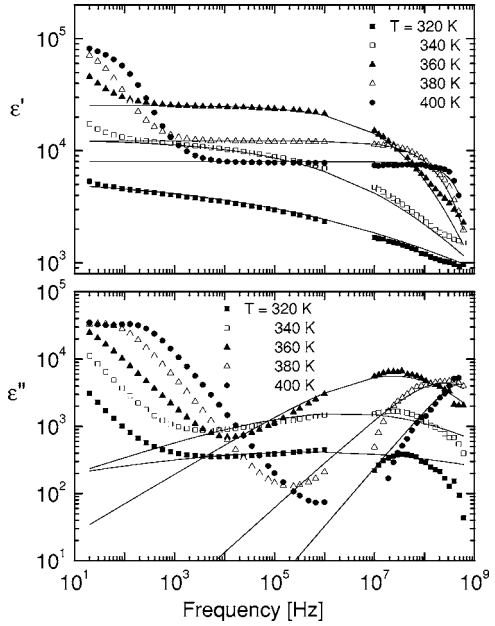

FIG. 2. Frequency dependence of the real (a) and imaginary parts (b) of the dielectric permittivity of unpoled SBN:Co at different temperatures with Havriliak-Negami functions best-fitted at high frequencies (solid lines).

cursors at $T>T_c$ and of spontaneous polarization at $T<T_c$, respectively.[22] In the latter study signatures of a crossover from 3D Ising to 3D RFIM criticality were reported.[23]

In order to confirm the RFIM nature of SBN the present study[24] is aimed at exploring the dynamical susceptibility at high frequencies f up to 1 GHz, which gives information about the dynamics of polar nanoregions and their crossover into the activated dynamic scaling regime close to T_c. Further, we investigate the change of the dynamic behavior of the polar nanoregions when applying an electric field upon cooling [field cooling (FC)]. It is expected that a homogeneous external field should weaken the RF's (Ref. 25) and thus reduce polydispersivity. The pertinent property to be explored is the distribution function of relaxation times, $g(\tau)$, within the concept of dynamic heterogeneity which is assumed to apply to a dynamic cluster system like SBN.

II. EXPERIMENTAL PROCEDURE

The measurements were carried out on congruently melting $Sr_{0.61}Ba_{0.39}Nb_2O_7$ (SBN61) doped with 0.002 wt % Co_3O_4, henceforth denoted as SBN:Co. Co doping is known to weakly enhance the relaxor properties of pure SBN.[26] Large and clear optical-quality single crystals were grown by the Czochralski technique. Rectangular-shaped sample with dimensions $6\times6\times0.7$ mm^3 were cut with the polar c axis normal to the large planes and polished to optical quality. In order to enhance the relaxor properties,[17,27] the samples were annealed without electrodes at 873 K for 2 h and then slowly cooled to room temperature at a cooling rate $\dot{T}=-30$ K/h. Silver paste was used to cover the major faces with electrodes. Prior to each measurement carried out on cooling, the samples were annealed at 450 K for 1 h in order to warrant identical conditions for all measurements and to eliminate memory effects of previous treatments. Real and imaginary parts of the dielectric permittivity were measured at frequencies between 20 Hz and 1 GHz (data points between 1 and 10 MHz are partially omitted because of piezoelectric resonance interference) by using a HP4284A impedance analyzer and a homebuilt coaxial dielectric spectrometer (frequency range from 1 MHz to 4 GHz).[28] By virtue of this latter spectroscopy the frequency range used previously[21] was significantly extended. At high frequencies, the complex permittiv-

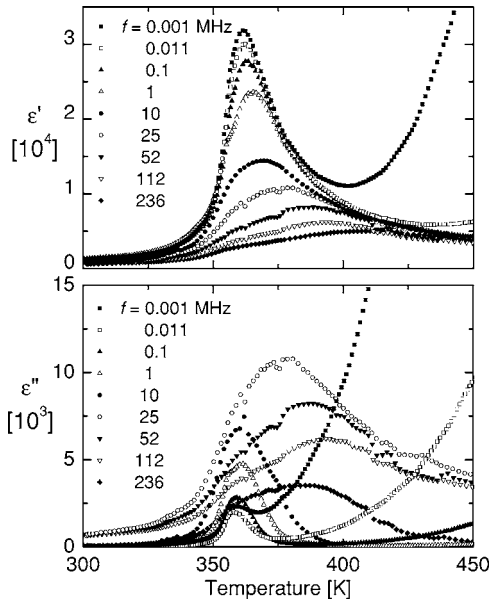

FIG. 3. Temperature dependence of the real and imaginary parts of dielectric permittivity of SBN:Co poled with $E=250$ kV/m at different frequencies.

ity $\varepsilon^* = \varepsilon' - i\varepsilon''$ was calculated taking into account the inhomogeneous distribution of the microwave field in the sample.[28] The cooling rates were typically $\dot{T} = -4$ K/h.

One set of measurements was performed without applying any bias field [upon ZFC after zero-field heating (ZFH)], while in the other set of measurements the sample was measured on heating after being cooled down with a bias field (FC).

III. EXPERIMENTAL RESULTS

Figure 1 shows results of measurements of the dielectric response of SBN, $\varepsilon^*(T)$, at different frequencies. At high temperatures, $T > 400$ K, and low frequencies, $f < 1$ MHz, the contribution of ionic conductivity can be seen as a monotonically increasing tail, while at $T \lessapprox 340$ K—i.e., below T_c—both components of $\varepsilon^*(T)$ are rapidly decreasing as a consequence of the ferroelectric phase transition. The extremely high ($\varepsilon'_{\max} \approx 2.8 \times 10^4$) and fairly large [full width at half maximum (FWHM) $\approx$40 K] low-frequency peak at $T_c \approx 348$ K (Ref. 26) is considered to reflect criticality,[29] although the typical RFIM rounding due to nonequilibrium[18] cannot easily be distinguished from ordinary relaxor behavior.[1] The dielectric dispersion observed at temperatures below 400 K (Fig. 2) is essentially characterized by two broadened dispersion steps in $\varepsilon'(f)$ and the corresponding broad peaks in $\varepsilon''(f)$. The steps become smeared and the peaks nearly indistinguishable at $T < T_c$. The low-f features can be attributed to conductivity and partially, at least at $T < T_c$, by domain wall creep, as discussed earlier,[30] while those at higher frequencies $f > 10^3$ Hz are attributed to domain wall relaxation. While the low-f data have been the subject of various of our previous papers,[21,23,30] in this paper we discuss primarily the latter contribution, which converts into relaxation modes of polar nanoregions at $T > T_c$.[30]

A poled sample shows very similar temperature (Fig. 3) and frequency (Fig. 4) dependences as compared to the unpoled sample. Differences are best seen in $\varepsilon''(f)$, which decreases upon poling at intermediate frequencies $f \approx 10^5$ Hz by more than one order of magnitude. These results actually confirm the results obtained previously,[30] albeit in a much broader frequency range.

Usually such broad dielectric dispersion is very difficult to fit with empirical models, such as those denoted by Cole-Cole or Havriliak-Negami.[31] In particular, the diffuse dielectric spectrum at low temperatures does not allow proper estimates of the relaxation times using conventional relaxation models or empirical equations. A special algorithm (*Tikhonov regularization*[32]) has been developed to solve this problem.

The original program performs the direct calculation of the distribution function $g(\tau)$ of the relaxation times from the complex dielectric permittivity at fixed temperatures versus frequency assuming a superposition of Debye-type processes (i.e., *dynamical heterogeneity*):

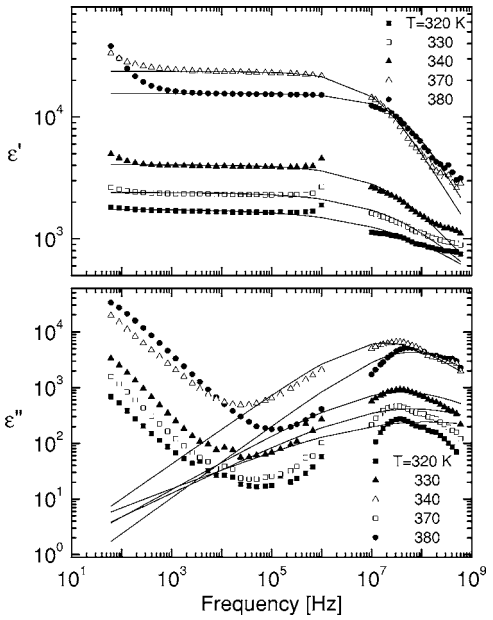

FIG. 4. Frequency dependence of the real and imaginary parts of dielectric permittivity of SBN:Co poled with $E = 250$ kV/m at different temperatures with Havriliak-Negami functions best-fitted at high frequencies (solid lines).

$$\varepsilon'(\omega) = \varepsilon_\infty + \int_0^\infty \frac{g(\tau)}{1 + (\omega\tau)^2} d(\ln \tau),$$
$$\varepsilon''(\omega) = \int_0^\infty \frac{(\omega\tau) g(\tau)}{1 + (\omega\tau)^2} d(\ln \tau). \tag{1}$$

The high-frequency limiting value ε_∞ and the total contribution of the dipoles to the permittivity $\Delta\varepsilon = \int g(\tau) d(\ln \tau)$ can be either given together with the initial data or defined during the solution. The basic integral transformations, Eq. (1), can be presented as the linear matrix equation

$$\mathbf{AX} = \mathbf{T}, \tag{2}$$

where the components of the matrix $\mathbf{A}$ are obtained by proper discretization of the integral transformation kernels. The components of the vectors $\mathbf{T}$ and $\mathbf{X}$ correspond to discretized values of the dielectric permittivity (as initial data) and to the distribution of relaxation times (as the result), respectively. Equation (2) is an ill-posed problem and cannot be solved straightforwardly. It is replaced by the following minimization problem:

$$\Phi = \|\mathbf{T} - \mathbf{AX}\| + \alpha \|\mathbf{RX}\|, \tag{3}$$

where α is the regularization parameter and $\mathbf{R}$ is the regularization matrix, which corresponds to the second derivative $g''(\tau)$. The conditions about the non-negative spectrum of the components of $g(\tau)$ are added as constraints. This constrained regularized minimization problem is solved by a least-squares technique making use of a simplified version of the program CONTIN originally developed by Provencher[33] and later adapted to dielectric spectra.[34]

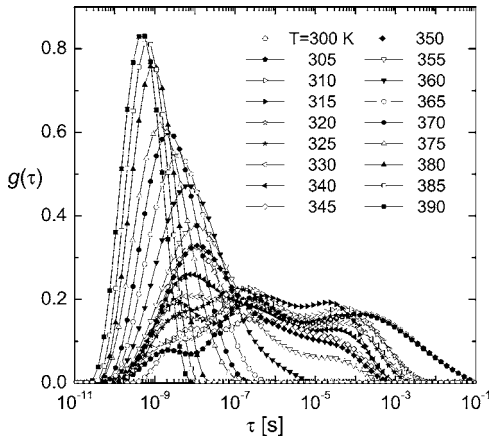

FIG. 5. Distribution of the relaxation times $g(\tau)$ at different temperatures of unpoled SBN:Co.

The real distribution function of the relaxation times of the SBN:Co crystal calculated from the experimental dielectric results (Fig. 2) is shown in Fig. 5. The regularization parameter $\alpha=5$ was found to be optimal. At $T\approx 380$ K, where the response of the nanoregions enters our experimental frequency window on cooling, the distribution of the relaxation times is symmetrically shaped. It is determined from those data, which are satisfactorily modeled by a Cole-Cole-type function $\varepsilon^*(\omega)=\varepsilon_\infty+\Delta\varepsilon/[1+(i\omega\tau)^\alpha]$, $\alpha<1$, in Fig. 2 (solid lines). At lower temperatures, the distribution of the relaxation times becomes asymmetrically shaped and rather refers to a Havriliak-Negami function $\varepsilon^*(\omega)=\varepsilon_\infty+\Delta\varepsilon/([1+(i\omega\tau)^\alpha])^\gamma$, $\gamma>1$, which is used to model the original data (solid lines). On further cooling to below T_c the distribution becomes very broad and contains several maxima, which are probably due to the freezing of the systems into domains. With the decrease of the temperature it broadens to the long

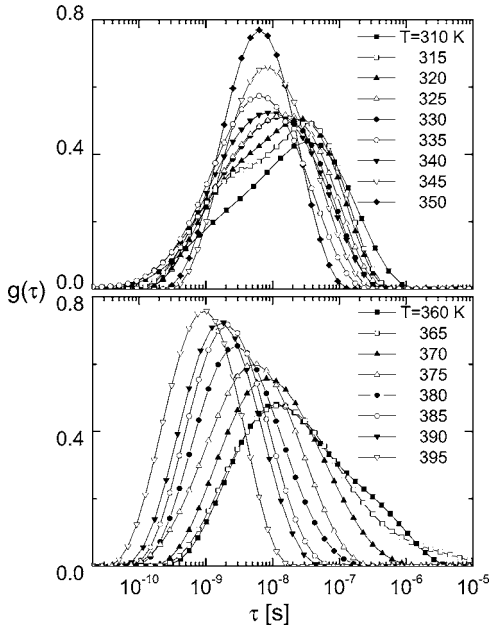

FIG. 6. Distribution of the relaxation times $g(\tau)$ at different temperatures of SBN:Co poled with $E=250$ kV/m.

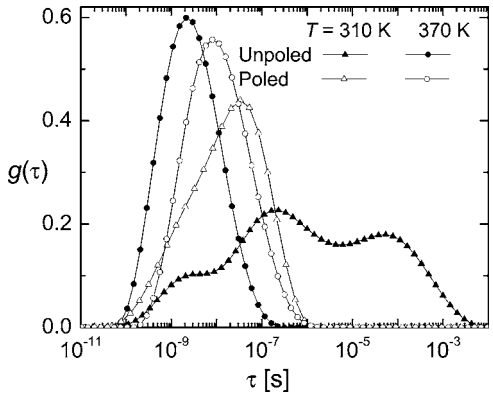

FIG. 7. Comparison of the distribution functions of relaxation times, $g(\tau)$, of poled and unpoled samples of SBN:Co at different temperatures.

relaxation times and indicates a strong increase of intercluster correlations. Also, its contribution to the permittivity increases at lower temperatures.

The distribution of relaxation times in the poled sample looks totally different (Fig. 6) when compared to the ZFC one (Fig. 5). With decreasing temperature it does not broaden significantly, the peak of the distribution shifts only slightly to longer relaxation times, and additional peaks are lacking for $T<T_c$. These differences can be most clearly seen in a comparison of the ZFC and FC distribution functions at $T=310$ and 370 K, respectively (Fig. 7).

IV. DISCUSSION

The shift of the distribution function $g(\tau)$ for the unpoled sample is most drastic at its low-frequency side, where the largest relaxation times of the system are located. As seen in Fig. 5 the displacements are huge between $T=365$ and 350 K, where the phase transition is approached. Here the activated dynamic scaling regime is encountered, which becomes more evident in a semilogarithmic plot, $^{10}\log(\tau_{\max}/\mathrm{s})$ vs T, in Fig. 8. A best fit to the activated scaling law[20]

$$\tau_{\max}=\tau_0\exp[(T_0/\{T-T_c\})^{\theta\nu}] \tag{4}$$

yields the parameters $\tau_0=(2.5\pm1.0)\times10^{-11}$ s, $T_0=(121\pm15)$ K, $T_c=(323\pm20)$ K, and $\theta\nu=1.32\pm0.31$. The ex-

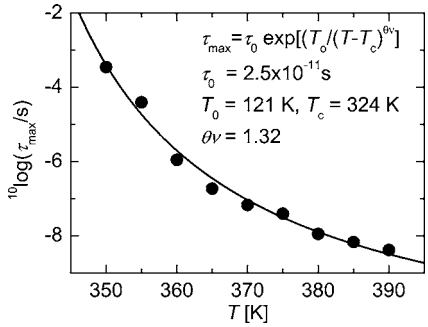

FIG. 8. Temperature dependence of the largest relaxation time $\tau_{\max}$ of $g(\tau)$ of unpoled SBN:Co (Fig. 5) best fitted to the activated dynamic scaling function, Eq. (4) (solid line; see text)

trapolated transition temperature T_c lies significantly below the value estimated by inspection of the original $\varepsilon^*(T)$ data (Fig. 1), $\approx$348 K.[26] Obviously, the critical slowing down continues to very low frequencies, which were not accessible in the present experiments.

The shortest relaxation time referring to small cluster relaxations at high temperatures, τ_0, is compatible to a very recent Vogel-Fulcher analysis of high-f dielectric data of pure SBN, which yield $f_\infty = 1.4 \times 10^{10}$ Hz; hence, $\tau_0 = (2\pi f_\infty)^{-1} = 1.1 \times 10^{-11}$ s.[35] In this study Eq. (4) has been modified by setting $\theta\nu \equiv 0$ and fitted to the peaks of $\varepsilon''(f)$. Hence, the dynamics of SBN was tacitly considered to be glass like, although further justification was not provided for this assertion. Here we stress that our analysis refers to the decisive largest relaxation time $\tau_{\max}$ (Ref. 20) rather than to the most probable one τ_m. Further, the exponent clearly turns out to be distinct from unity, $\theta\nu > 1$, in favor of the correct RFIM scaling law, Eq. (4). Hence, careful inspection shows that the empirical Vogel-Fulcher law does not apply to RFIM transitions as was stressed already in the pioneering study of the RF nature of relaxors.[12]

As shown in Fig. 7 an external electric field obviously suppresses either the fastest (at high T—viz., 370 K) or the slowest relaxation times (at low T—viz, 310 K) in the poled sample, when compared to the spectra of freely fluctuating polar nanoregions (high T) and random ferroelectric polar nanodomains (low T), respectively, of unpoled SBN:Co. On the one hand, the observed *slowing down* in the paraelectric regime is probably due to reduced restoring forces, which are probed by the nanoregions under the external field. This may be explained as follows. A homogeneous field is known to weaken the RF's (Ref. 25) and thus to weaken the fluctuation controlled RF pinning forces onto the clusters. As a consequence the average size of the nanoregions grows as the RF's decrease.[25,36] This in turn enhances their "moments of inertia" and thus their relaxation times. On the other hand, the observed *speeding-up* in the ferroelectric state after poling is due to the polar homogeneity after FC. The single-domain state thus created simply lacks the typical fractal domain landscape[37] exhibiting a rich low-f wall-induced relaxation spectrum.[21]

V. CONCLUSION

Measurements of the dielectric relaxation of SBN:Co at frequencies up to the GHz range have clearly shown that the paraelectric regime $T > 348$ K is controlled by polar nanoregions, which reveal activated critical dynamics when approaching T_c. The enormous slowing down must not be confounded with freezing into a generic glass state. Field cooling causes weakened RF's in the paraelectric range and thus a slower dynamics, while the absence of nanopolar domains in the homogeneously poled ferroelectric phase invalidates the low-f relaxational degrees of freedom and thus sharpens the relaxation spectrum.

ACKNOWLEDGMENTS

Thanks are due to R. Pankrath (University of Osnabrück) for providing the excellent single-crystal samples of SBN:Co. This work was supported by the Deutsche Forschungsgemeinschaft (DFG) within the framework of Schwerpunktprogramm "Strukturgradienten in Kristallen."

*Electronic address: kleemann@uni-duisburg.de

[1] G. A. Smolenskii and V. A. Isupov, Dokl. Akad. Nauk SSSR **97**, 653 (1954).
[2] X. Yao, Z. L. Chen, and L. E. Cross, J. Appl. Phys. **54**, 3399 (1984).
[3] L. E. Cross, Ferroelectrics **76**, 241 (1987).
[4] G. A. Samara, J. Phys.: Condens. Matter **15**, R367 (2003); W. Kleemann, G. A. Samara, and J. Dec, in *Polar Oxides—Properties, Characterization, and Imaging*, edited by R. Waser, U. Böttger, and S. Tiedke (Wiley-VCH, Weinheim, 2005), p. 275.
[5] B. E. Vugmeister and H. Rabitz, Phys. Rev. B **57**, 7581 (1998); **61**, 14448 (2000).
[6] Ang Chen, Yu Zhi, and Jing Zhi, Phys. Rev. B **61**, 957 (2000).
[7] U. Bianchi, J. Dec, W. Kleemann, and J. G. Bednorz, Phys. Rev. B **51**, 8737 (1995).
[8] S. A. Prosandeev, W. Kleemann, and J. Dec, J. Phys.: Condens. Matter **13**, 5957 (2001).
[9] R. B. Griffiths, Phys. Rev. Lett. **23**, 17 (1969).
[10] G. Burns and F. H. Dacol, Ferroelectrics **104**, 25 (1990).
[11] Y. Imry and S. K. Ma, Phys. Rev. Lett. **35**, 1399 (1975).
[12] V. Westphal, W. Kleemann, and M. D. Glinchuk, Phys. Rev. Lett. **68**, 847 (1992); W. Kleemann, Int. J. Mod. Phys. B **7**, 2469 (1993).
[13] H. Qian and L. A. Bursill, Int. J. Mod. Phys. B **10**, 2027 (1996); A. K. Tagantsev and A. E. Glazounov, Phys. Rev. B **57**, 18 (1998).
[14] C. Stock, R. J. Birgeneau, S. Wakimoto, J. S. Gardner, W. Chen, Z.-G. Ye, and G. Shirane, Phys. Rev. B **69**, 094104 (2004).
[15] R. Blinc, J. Dolinsek, A. Gregorovic, B. Zalar, C. Filipic, Z. Kutnjak, A. Levstik, and R. Pirc, Phys. Rev. Lett. **83**, 424 (1999); R. Pirc and R. Blinc, Phys. Rev. B **60**, 13470 (1999).
[16] V. Bobnar, Z. Kutnjak, R. Pirc, R. Blinc, and A. Levstik, Phys. Rev. Lett. **84**, 5892 (2000).
[17] A. M. Glass, J. Appl. Phys. **40**, 4699 (1969); D. Viehland, Z. Xu, and W.-H. Huang, Philos. Mag. B **71**, 205 (1995); **71**, 219 (1995).
[18] W. Kleemann, J. Dec, P. Lehnen, R. Blinc, B. Zalar, and R. Pankrath, Europhys. Lett. **57**, 597 (2002).
[19] Y. Xu., Z. Li, W. Li, H. Wang, and H. Chen, Phys. Rev. B **40**, 11902 (1989).
[20] D. S. Fisher, Phys. Rev. Lett. **56**, 416 (1986); A. T. Ogielski and D. A. Huse, *ibid.* **56**, 1298 (1986).
[21] J. Dec, W. Kleemann, Th. Woike, and R. Pankrath, Eur. Phys. J. B **14**, 627 (2000).
[22] P. Lehnen, W. Kleemann, Th. Woike, and R. Pankrath, Eur. Phys. J. B **14**, 633 (2000).
[23] W. Kleemann, J. Dec, P. Lehnen, Th. Woike, and R. Pankrath, in

Fundamental Physics of Ferroelectrics, edited by R. E. Cohen, AIP Conf. Proc. No. 535 (AIP, Melville, NY, 2000), p. 26.

[24] A first report on this research was presented at the *Spring Meeting of the German Physical Society*, Regensburg, 2004 [Verh. Dtsch. Phys. Ges. 39, 2/88 (2004)].

[25] D. Andelman and J. F. Joanny, Phys. Rev. B **32**, 4818 (1985).

[26] P. Lehnen, E. Beckers, W. Kleemann, Th. Woike, and R. Pankrath, Ferroelectrics **253**, 11 (2001).

[27] R. Guo, A. Bhalla, G. Burns, and F. Dacol, Ferroelectrics **93**, 397 (1989).

[28] J. Grigas, *Microwave Dielectric Spectroscopy of Ferroelectrics and Related Materials* (OPA Gordon and Breach, Amsterdam, 1996).

[29] J. Dec, W. Kleemann, V. Bobnar, Z. Kutnjak, A. Levstik, R. Pirc, and R. Pankrath, Europhys. Lett. **55**, 781 (2001).

[30] W. Kleemann, J. Dec, S. Miga, Th. Woike, and R. Pankrath, Phys. Rev. B **65**, 220101(R) (2002).

[31] A. K. Jonscher, *Dielectric Spectroscopy* (Chelsea Dielectric Press, London, 1992).

[32] A. N. Tikhonov and V. Y. Arsenin, *Solution of Ill-posed Problems* (Winston, New York, 1977).

[33] S. W. Provencher, Comput. Phys. Commun. **27**, 213 (1982).

[34] J. Banys, S. Lapinskas, A. Kajokas, A. Matulis, C. Klimm, G. Völkel, and A. Klöpperpieper, Phys. Rev. B **66**, 144113 (2002).

[35] F. Buixaderas, M. Savino, M. Kempa, S. Veljko, S. Kamba, J. Petzelt, R. Pankrath, and S. Kapphan, J. Phys.: Condens. Matter **17**, 653 (2005).

[36] J. Villain, Phys. Rev. Lett. **52**, 1543 (1984).

[37] P. Lehnen, W. Kleemann, Th. Woike, and R. Pankrath, Phys. Rev. B **64**, 224109 (2001).